Computational studies of the laminar burning velocity of a producer gas and air mixture under typical engine conditions

G Sridhar, P J Paul and H S Mukunda
Combustion, Gasification, and Propulsion Laboratory, Department of Aerospace Engineering, Indian Institute of Science, Bangalore, India
The MS was received on 6 July 2004 and was accepted after revision for publication on 31 August 2004.
DOI: 10.1243/095765005X6917

Abstract

This paper discusses computational results concerning the laminar burning velocity of a biomass-derived producer gas and air mixture at pressures and temperatures typical of the unburned mixture in a reciprocating engine. The computations are based on solving conservation equations describing laminar one-dimensional, multi-component, chemically reacting, and ideal gas mixtures that have been formulated by earlier researchers. Based on a number of calculations at varying initial pressures and temperatures, and equivalence ratios, an expression for estimating the laminar burning velocity with the recycled gas mass fraction has been obtained. Also, the effect of varying amounts of recycled gas on the burning velocity has been determined. These data on laminar burning velocities will be useful in predicting the burnrate in a sparkignition (SI) engine fuelled with a producer gas and air mixture.

Keywords: laminar burning velocity, producer gas, recycled gas

1. INTRODUCTION

The laminar burning velocity is an important intrinsic property of combustible fuels and of air and burned gas mixtures. It is the velocity at which the flame propagates into a quiescent premixed unburned mixture ahead of the flame. In the case of reciprocating internal combustion engines, an additional feature is the presence of residual or burned gas from the earlier cycle, and this causes a reduction in the laminar burning velocity [1]. The study of laminar burning velocity becomes relevant for estimating the burn rate in a spark ignition (SI) engine. Laminar burning velocities at pressures and temperatures typical of reciprocating engine operation are usually measured using spherical closed vessels. Data and derived correlations are available in the literature for a wide range of premixed air and fuel containing hydrogen, methane, propane, iso-octane, methanol, and gasoline [1]. However, there have been few studies using producer gas fuel, either computational or experimental (at ambient conditions), and there are no studies reported at pressures and temperatures that are typically encountered in an SI engine. This paper discusses the computational results for a producer gas þ air mixture under thermodynamic conditions typical of a reciprocating engine, with and without recycled gas. The code that is employed for computation has been validated against experimental results for the same fuel–air mixture at ambient conditions. The results are expected to help in understanding if the optimum ignition timing for producer gas operation is advanced/retarded with respect to that of an engine fuelled with natural gas. Also, the data that are available in the form of generalized correlations are useful in predicting the burnrate in an SI engine

fuelled with a producer gas þ air mixture [2, 3].

2 EARLIER STUDIES

2.1 Experimental

The laminar burning velocity for a producer gas + air mixture has been obtained by experiments and theoretical calculations for various compositions and mixture ratios by earlier researchers [4–6]. The laminar burning velocity at ambient conditions (0.92 kPa, 300 K) has been experimentally determined by Kanitkar et al. [4] by conducting experiments using standard flame tube apparatus for producer gas + air mixtures for a wide range of mixture ratios. These experiments were conducted under laboratory reference conditions using producer gas generated from an online Indian Institute of Science (IISc) open to preburn gasification system. The gas consisted of 18–23% H_2, 17–20% CO, 3–4%CH_4, 13–14% CO_2, and balance N_2. A wide range of mixture ratios was considered within the flammability limits of rich and lean mixtures, namely the equivalence ratio ϕ=0.47 (26 vol % fuel) and 1.65 (56 vol % fuel) for lean and rich limits respectively. The physical values of burning velocity varied between 0.10 and 0.13 m/s from lean to rich limits, the peak value being 0.50+0.05 m/s around stoichiometry (45 vol % fuel). The burning velocity for the producer gas þ air mixture is found to be 30 per cent higher compared with the stoichiometric CH_4 + air mixture at ambient conditions, with comparatively higher values at the lean limit (CH_4 ~ 0.025 m/s).

2.2 Theoretical predictions

2.2.1 Procedure

Theoretical laminar burning velocity predictions have been made by earlier researchers [5–8] using in-house developed 'FLAME CODE' software for a one-dimensional adiabatic premixed laminar flame. The calculations involve the solution of conservation equations describing the laminar one-dimensional multi-component, chemically reacting, and ideal gas mixtures. The relevant conservation equations are

$$\frac{\partial \rho}{\partial t} + \frac{\partial (\rho u)}{\partial x} = 0 \tag{1}$$

$$\rho \frac{\partial Y_i}{\partial t} + \rho u \frac{\partial Y_i}{\partial x} = -\frac{\partial J_i}{\partial x} + \dot{\omega}_i''', \qquad i = 1, \ldots, N_s \tag{2}$$

$$\rho \frac{\partial h}{\partial t} + \rho u \frac{\partial h}{\partial x} = \frac{\partial}{\partial x}\left(\frac{\lambda}{c_p}\frac{\partial h}{\partial x}\right) - \sum_{i=1}^{N_s} \frac{\partial}{\partial x}\left[h_i\left(J_i + \frac{\lambda}{c_p}\frac{\partial Y_i}{\partial x}\right)\right] \tag{3}$$

where x is the coordinate fixed to the laboratory normal to the flame, Y_i are the mass fractions of the species, ω''' is the volumetric production/consumption rate of chemical species, and h is the sum of chemical and sensible enthalpies given by

$$h = \sum_{i=1}^{N_s} \left(h_i^0 + \int_{T_0}^{T} c_{pi}\, \mathrm{d}T\right) Y_i \tag{4}$$

The corresponding boundary conditions are given by

$$\begin{aligned} &x \longrightarrow -\infty : \frac{\partial Y_i}{\partial x} \longrightarrow 0, \quad \frac{\partial T}{\partial x} \longrightarrow 0 \\ &x \longrightarrow +\infty : Y_i \longrightarrow Y_{i,\mathrm{u}}, \quad T \longrightarrow T_{\mathrm{u}} \end{aligned} \tag{5}$$

As noted in equation (5), the hot boundary contains the equilibrium mass fractions of the relevant species and the adiabatic flame temperature, and the cold boundary contains the reactant mass fractions and the ambient temperature. The calculations commence from a given set of initial profiles of mass fraction, Y_i and temperature, T, which are linearly distributed with distance x over an assumed flame thickness. The choice of the set of kinetic studies and rate constants has been arrived at by earlier researchers [6, 8]. This is a set of elementary reactions validated for H_2–air and CH_4–air systems. The CO–air system forms a subset of the CH_4–air system. With the producer gas representing the CO–H_2–CH_4–O_2–N2 system, the species and the reactions considered for calculations are given in Table 1.
The reaction rate is defined as

$$\frac{dC_i}{dt} = A_f e^{-E/RT} T^m \prod C_j^{\nu_j} \quad (6)$$

where C_i is the concentration of species and ν_j are the stoichiometric coefficients of the reactions listed in Table 1. The values of frequency factor A_f, activation energy E, and coefficient m are given in Table 1. For each species, the NASA polynomial cure fits are used to calculate the thermodynamic properties, namely specific heat, enthalpy, and entropy. The transport properties such as diffusion coefficients and thermal conductivity for the mixture are evaluated using the correlations given in the report by Brokaw [9]. The diffusive fluxes are calculated using trace diffusion approximation neglecting the Soret and Dufour effects. The conservation equations are solved by a finite difference scheme using the operator-split technique. In this method the reaction equation is solved using an implicit method of the Crank–Nicholson type and the diffusion equation is solved using the explicit forward-time central space (FTCS) scheme. The set of equations are solved at one time level and the properties at the next time level are obtained by a simple updating scheme. The burning velocities for different species are calculated, and the convergence of these burning velocities as well as the time of integration is used to determine the steady state. The results of burning velocity along with Y_i and T constitute the output of the solution procedure.

Table 1 Kinetic scheme used for the present laminar burning velocity calculations [10]

Number	Reaction	A_f (cm^3/s mol)	m	E (kcal/mol)
R1	$OH + O \leftrightarrow O_2 + H$	1.8E+13	0.0	0.0
R2	$O + H_2 \leftrightarrow OH + H$	1.5E+07	2.0	76.58
R3	$OH + H_2 \leftrightarrow H_2O + H$	1.0E+08	1.6	33.28
R4	$OH + OH \leftrightarrow H_2O + O$	1.5E+09	1.14	0.0
R5	$H + H + M \leftrightarrow H_2 + M^*$	9.7E+16	−0.6	0.0
R6	$H + OH + M \leftrightarrow H_2O + M$	2.2E+22	−2.0	0.0
R7	$O + O + M \leftrightarrow O_2 + M$	2.9E+17	−1.0	0.0
R8	$H + O_2 + M \leftrightarrow HO_2 + M$	2.0E+18	−0.8	0.0
R9	$H + HO_2 \leftrightarrow OH + OH$	1.5E+14	0.0	10.80
R10	$H + HO_2 \leftrightarrow H_2 + O_2$	2.5E+13	0.0	73.17
R11	$O + HO_2 \leftrightarrow OH + O_2$	2.0E+13	0.0	0.0
R12	$OH + HO_2 \leftrightarrow H_2O + O_2$	2.0E+13	0.0	0.0
R13	$HO_2 + HO_2 \leftrightarrow H_2O_2 + O_2$	2.0E+12	0.0	0.0
R14	$OH + OH + M \leftrightarrow H_2O_2 + M$	3.3E+22	−2.0	0.0
R15	$H + H_2O_2 \leftrightarrow H_2 + HO_2$	1.7E+12	0.0	37.4
R16	$H + H_2O_2 \leftrightarrow H_2O + OH$	1.0E+13	0.0	36.1
R17	$O + H_2O_2 \leftrightarrow OH + HO_2$	2.8E+13	0.0	64.35
R18	$OH + H_2O_2 \leftrightarrow H_2O + HO_2$	7.0E+12	0.0	14.03
R19	$CO + H + M \leftrightarrow CHO + M$	6.9E+14	0.0	17.0
R20	$CO + O + M \leftrightarrow CO_2 + M$	7.1E+13	0.0	−45.11
R21	$CO + OH \leftrightarrow CO_2 + H$	4.4E+07	1.5	−74.1
R22	$CO + HO_2 \leftrightarrow CO_2 + OH$	1.5E+14	0.0	24.0
R23	$CO + O_2 \leftrightarrow CO_2 + O$	2.5E+12	0.0	48.15
R24	$CH_4 + H \leftrightarrow CH_3 + H_2$	2.2E+04	3.0	87.61
R25	$CH_4 + O \leftrightarrow CH_3 + OH$	1.2E+07	2.10	76.28
R26	$CH_4 + OH \leftrightarrow CH_3 + H_2O$	1.6E+06	2.10	24.76
R27	$CH_4 + M \leftrightarrow CH_3 + H + M$	5.7E+17	0.0	92.24
R28	$CH_3 + O \leftrightarrow CH_2O + H$	7.0E+13	0.0	0.0
R29	$CH_3 + O_2 \leftrightarrow CH_2O + O + H$	1.5E+13	0.0	29.7
R30	$CH_2O + H \leftrightarrow CHO + H_2$	2.5E+13	0.0	40.40
R31	$CH_2O + O \leftrightarrow CHO + OH$	3.5E+13	0.0	35.38
R32	$CH_2O + OH \leftrightarrow CHO + H_2O$	3.0E+13	0.0	12.03
R33	$CH_2O + CH_3 \leftrightarrow CHO + CH_4$	1.0E+11	0.0	61.64
R34	$CH_2O + M \leftrightarrow CHO + H + M$	1.4E+17	0.0	76.85
R35	$CH_2O + M \leftrightarrow CO + H_2 + M$	2.0E+16	0.0	38.0
R36	$CHO + H \leftrightarrow CO + H_2$	2.0E+14	0.0	0.0
R37	$CHO + O \leftrightarrow CO + OH$	3.0E+13	0.0	0.0
R38	$CHO + O \leftrightarrow CO_2 + H$	3.0E+13	0.0	0.0
R39	$CHO + OH \leftrightarrow CO + H_2O$	5.0E+13	0.0	0.0
R40	$CHO + O_2 \leftrightarrow CO + HO_2$	3.0E+12	0.0	0.0

*M represents the third body, which is the chaperon efficiency weighted total concentration.

The burning velocity is calculated from

$$S_{L,i} = \frac{\int_{-\infty}^{+\infty} \dot{\omega}_i''' \, dx}{\rho_u (Y_{i,u} - Y_{i,b})}, \qquad i = 1, 2, \ldots, N_s \tag{7}$$

$$S_{L,T} = \frac{\int_{-\infty}^{+\infty} \sum_{i=1}^{N_s} \dot{\omega}_i''' h_i^o \, dx}{\rho_u (H_u - H_b)} \tag{8}$$

where Hu and Hb are the total enthalpy of the unburned mixture and burned gases respectively.

2.2.2 Predictions – high pressure

In an earlier study [5] conducted using the above code for a producer gas þ air mixture at ambient conditions, the theoretical predictions compared well within the error band of experimental data. In a subsequent study [6], predictions at higher pressures indicated the burning velocity of producer gas to decrease from 0.4 m/s at 1 atm (300 K) to 0.04 m/s at 40 atm (300 K). Such a drastic reduction in burning velocity at high pressure was attributed to the drastic reduction in the radical pool owing to suppression of dissociation. This drastic reduction in burning velocity at higher pressure has relevance in the field of the internal combustion engine because of the similar pressures encountered during operation. However, this effect can be expected to be completely modified by the corresponding increase in temperature on account of the compression in a reciprocating engine.

3 CURRENT WORK – HIGH PRESSURE AND TEMPERATURE ALONG WITH RECYCLED GAS

For the purpose of calculations, a nominal composition with 20% H_2, 20% CO, 2% CH_4, 12% CO_2, and balance N_2 was considered. In addition, recycled gas (burned gas) was considered in varying amounts to simulate the actual air–fuel conditions in a

Table 2 Computational laminar burning velocities at varying initial conditions of the mixture – pressure, temperature, and recycled gas (RG) mass fraction

		S_L (cm/s)						
		Case I*	Case II†					
		$\Phi = 0.90$	$\Phi = 1.07$			$\Phi = 0.90$		
Pressure, bar (abs)	$T_{unburned}$ (K)	0% RG	0% RG	5% RG	10% RG	0% RG	5% RG	10% RG
5	630	105	143	130	112	122	110	92
10	746	132	179	162	139	154	144	113
15	821	151	205	183	159	176	151	132
20	876	163	217	196	169	189	166	141
25	920	173	229	205	176	200	174	148
30	954	178	236	207	180	206	180	152
35	995	191	249	213	186	221	190	164
40	1028	202	259	231	189	227	198	176
45	1056	207	268	238	200	235	208	181
50	1082	215	275	245	204	243	214	190

*Case I corresponds to H_2 = 20%, CO = 18%, CH_4 = 2%, CO_2 = 12%, and balance N_2.
†Case II corresponds to H_2 = 20%, CO = 20%, CH_4 = 2%, CO_2 = 12%, and balance N_2.
Recycled gas for case I and II is H_2O = 12%, CO_2 = 15%, and balance N_2.

reciprocating engine. In fact, in a reciprocating engine there is some amount of burned product that is trapped in the clearance volume from the previous cycle, and also some amount of reverse flow of burned products from the cylinder into the intake manifold. The extent or fraction of recycled gas in the fresh mixture depends upon the compression ratio and the valve overlap period [1]. In order to simulate the mixture conditions close to actual SI engine operation, varying amounts of recycled gas fraction (0–10 per cent) are considered. Calculations are made at varying equivalence ratios ϕ, initial temperatures, and initial pressures, and with varying amounts of recycled gas: 0, 5, and 10 per cent. Adiabatic temperature corresponding to each pressure is considered for the unburned mixture. The results of these computations are shown in Table 2 for two identified producer gas þ air mixtures and at two equivalence ratios. It is clear from the above data that burning velocities decrease substantially with dilution at all initial mixture pressure conditions and ϕ. This essentially occurs owing to reduction in the adiabatic flame temperature as a result of dilution. The effect of dilution on the burning velocity is shown in Fig. 1 for rich and lean fuel þ air mixtures at

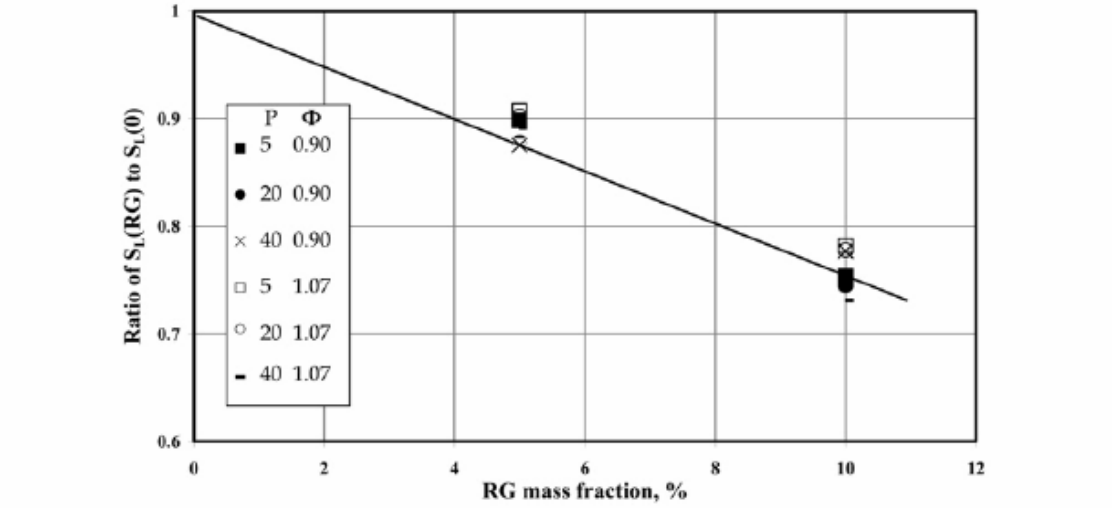

Fig. 1 Effect of variation in recycled gas (RG) on the laminar burning velocity at rich and lean mixtures and different initial pressures

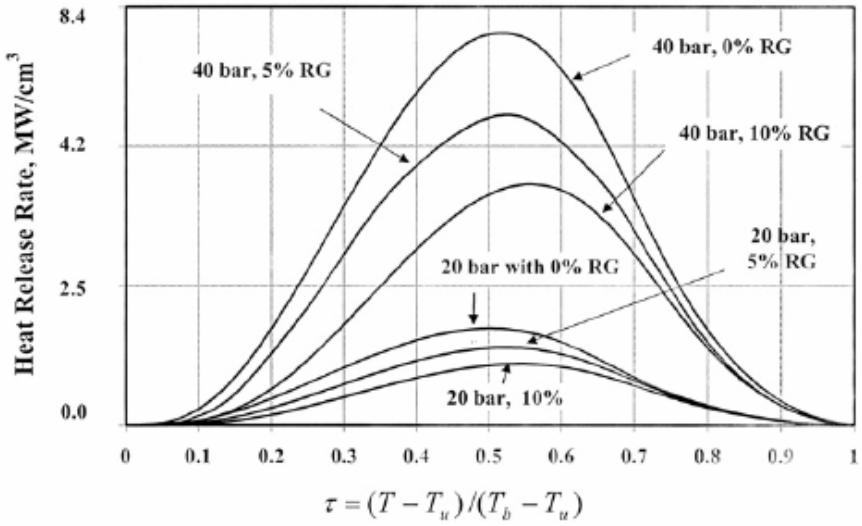

Fig. 2 Heat release rate profile versus non-dimensional temperature across the flame at two initial mixture pressures of 20 and 40 bar (abs), with and without recycled gas (RG)

different initial mixture pressures. The proportional reduction in laminar burning velocity is essentially independent of the unburned mixture equivalence ratio, initial pressure, and initial temperature over the range of computations conducted. This effect is consistent with studies carried out by Rhodes and Keck [11] using gasoline fuel at initial pressures of 1 and 2 atm.

A least-squares curve fitting done using the data of case II resulted in an expression for laminar burning velocity in terms of cylinder pressure

$$S_L(\mathrm{cm/s}) = 94.35\left(\frac{p}{p_0}\right)^{0.2744}[0.96 + 1.2(\Phi - 1)] \times (1 - 2.4\psi) \quad (9)$$

where p is the pressure in bar (abs), p_o is the reference pressure (1.0 bar), Ψ is the recycled gas mass fraction, and ϕ is the fuel–air equivalence ratio. The burning velocity dependence upon the initial temperature is built into the pressure term in equation (9). The above correlation is correct within +6 per cent for the data of case II. This correlation fits for the data in case I by including a correction factor for the lower CO content, which is explained below.

The burning velocity of producer gas is quite sensitive to variations in H_2 and CO fraction, and this is quite possible in the process of gasification. A sensitivity analysis of variation in CO and H_2 content towards laminar burning velocity at an equivalence ratio of about 0.9 revealed the burning velocity to decrease by about 7 per cent for every 1 per cent reduction in H_2 or CO content. When this correction is made, equation (9) is modified as follows

$$S_L(\mathrm{cm/s}) = 94.35\left(\frac{p}{p_0}\right)^{0.2744}[0.96 + 1.2(\Phi - 1)] \times (1 - 2.4\psi)(1 - 7(0.2 - X_{H_2}) \times [1 - 7(0.2 - X_{CO}] \quad (10)$$

Equation (10) is valid for an H_2 or CO content between 18 and 20 per cent. To explore further the behavior seen above, the heat release rate is examined at six varying conditions. The conditions examined correspond to 40 and 20 bar (abs) initial pressure with 0, 5, and 10 per cent recycled gas fraction. The heat release rate across the flame is plotted as a function of non-dimensional temperature for six conditions in Fig. 2. The initial unburned gas temperature and the corresponding adiabatic flame/burned gas temperatures are given in Table 3. The influence of RG on the heat release rate at both initial mixture pressures is very evident for the plot.

The distance between positions of 1 per cent (initial temperature, T_u) and 99 per cent (adiabatic flame/burned gas temperature, T_{ad} or T_b) temperature rise is used for estimation of the flame thickness, δ_L, and is shown in Table 3. The δ_L is about 0.21+0.02 mm and 0.11+0.02 mm at 20 and 40 bar (abs) pressure respectively. The order of flame thickness is well within the values measured experimentally by Smith [12] of ~ 0.2 mm for propane fuel under engine conditions. Similarly, the flame thickness according to the procedure of Abraham et al. [13] (ratio of thermal diffusivity to laminar burning velocity) works out at about 0.8 μm.The Kolmogorov length scale, l_k, for the engine under study is about 4 mm (for Re_T = 2100 and l_I = 1.2 mm, assuming isotropic and homogeneous turbulence: $lk = l_I Re_T^{-3/4}$). Therefore, the ratio of $l_k/d_L \approx 5.0$ for the flame can be treated as negligibly thin in the context of the wrinkled flame structure relevant to an SI engine [13].

Table 3 Laminar burning velocities and laminar flame thicknesses at $\Phi = 1.07$ for different pressures and recycled gas (RG). The fuel gas composition corresponds to case II at $\Phi = 1.07$

	20 bar (abs)			40 bar (abs)		
	0%RG	5%RG	10%RG	0%RG	5%RG	10%RG
T_u (K)	876	876	876	1028	1028	1028
T_b (K)	2330	2275	2200	2450	2395	2345
S_L (cm/s)	217	196	169	259	231	189
δ_L (mm)	0.23	0.21	0.19	0.092	0.13	0.09

4 CONCLUSION

Based on a number of calculations at varying initial pressures and temperatures, and equivalence ratios, an expression for estimating the laminar burning velocity with the recycled gas mass fraction has been derived. Also, the effect of dilution by varying the amount of recycled gas on the burning velocity has been determined. These data on laminar burning velocities will be useful in predicting the burn rate in a spark ignition engine fuelled with a producer gas þ air mixture.

REFERENCES

1 Heywood, J. B. Internal Combustion Engine Fundamentals, International edition, 1988 (McGraw-Hill).

2 Sridhar, G., Paul, P. J. and Mukunda, H. S. Experiments and modeling of producer gas based reciprocating engines. In Proceedings of 2002 Fall Technical Conference of ASME Internal Combustion Engines Division, New Orleans, Louisiana, 2002, ICE-Vol. 39, paper ICEF2002-520, pp. 377–388.

3 Sridhar, G. Experimental and modelling studies of producer gas based spark-ignited reciprocating engines. PhD thesis, Indian Institute of Science, 2003.

4 Kanitkar, S., Chakravarty, P., Paul, P. J. and Mukunda, H. S. The flame speeds, temperature and limits of flame propagation for producer gas–air mixtures – experimental results. The Proceedings of 4th National Meet on Biomass Gasification a nd Combustion, Mysore, India, 1993, Vol. 4, pp. 50–62 and Combustion, Mysore, India, 1993, Vol. 4, pp. 50–62.

5 Chakravarthy, P., Mishra, D. P., Paul, P. J. and Mukunda, H. S. The theoretical calculations of the limits of flame propagation for producer gas mixture. In Proceedings of 4th National Meet on Biomass Gasification and Combustion, 1993, Vol. 4, pp. 28–37.

6 Mishra, D. P., Paul, P. J. and Mukunda, H. S. Computational studies on the flame propagation in producer gas–air mixture and experimental comparisons. In Proceedings of XIII National Conference on IC Engines and Combustion, Bangalore, India, 1994, Vol. 13, pp.256–262. **Q1**

7 Goyal, G. Development and application of an efficient implicit–explicit method for one-dimensional premixed flames. PhD thesis, IISc, 1989.

8 Lakshmisha, K. N. Computational studies on the flammability limits of premixed gases. PhD thesis, IISc, 1991

9 Brokaw R. S. Alignment charts for transport properties, viscosity and diffusion coefficients for non-polar gases mixtures at low density. Technical report TRR-81, NASA, 1961.

10 Warnatz, J. Combustion Chemistry (Ed. W.C Gardiner), 1984, pp 197–360 (Springer-Verlag, New York).

11 Rhodes, D. B. and Keck, J. C. Laminar burning speed measurements of indolene–air-diluent mixtures at high pressures and temperature. SAE paper 850047, 1985, pp. 23–35.

12 Smith, J. R. Turbulent flame structure in a homogenous-charge engine. SAE paper 820043, 1982, Vol. 91, pp. 150–164.

13 Abraham, J., Williams, F. A., and Bracco, F. V. A discussion of turbulent flame structure in premixed charges. SAE paper 850345, 1985, Vol. 94, pp. 128–143.

APPENDIX: NOTATION

A_f	frequency factor
C_i	species concentration
E	activation energy
H	total enthalpy
IISc	Indian Institute of Science
J	mass flux
l_l	integral length scale
l_k	Kolmogorov length scale
p	pressure
RG	recycled gas
Re_T	turbulence Reynolds number
SI	spark ignition
S	burning velocity
t	time
T	temperature
u	velocity
v_j	stoichiometric coefficients
x	coordinate
X	mole fraction
Y_i	mass fraction
d	flame thickness
l	thermal conductivity
r	density
F	equivalence ratio
C	recycled gas mass fraction
ω'''	volumetric production /consumption rate

Subscript

b	burned
L	laminar
u	unburned